Novel, Potent Small-Molecule Inhibitors of the Molecular Chaperone Hsp90 Discovered through Structure-Based Design

Brian W. Dymock,[†] Xavier Barril,[†] Paul A. Brough,[†] Julie E. Cansfield,[†] Andrew Massey,[†] Edward McDonald,[‡] Roderick E. Hubbard,[†] Allan Surgenor,[†] Stephen D. Roughley,[†] Paul Webb,[†] Paul Workman,[‡] Lisa Wright,[†] and Martin J. Drysdale*[,†]

Vernalis Ltd., Granta Park, Great Abington, Cambridge CB1 6GB, U.K., and Cancer Research U.K. Centre for Cancer Therapeutics, The Institute of Cancer Research, 15 Cotswold Road, Sutton, Surrey SM2 5NG, U.K.

Received April 15, 2005

Abstract: The crystal structure of a previously reported screening hit **1** (CCT018159) bound to the N terminal domain of molecular chaperone Hsp90 has been used to design 5-amide analogues. These exhibit enhanced potency against the target in binding and functional assays with accompanying appropriate cellular pharmacodynamic changes. Compound **11** (VER-49009) compares favorably with the clinically evaluated 17-AAG.

Molecular chaperones are protein machines that are responsible for the correct folding, stabilization, and function of other proteins in the cell.[1] Exposure of cells to environmental stress, including heat shock, alcohols, heavy metals, and oxidative stress, results in the cellular accumulation of these chaperones, commonly known as heat shock proteins (Hsp's). Hsp90 has emerged over the past few years as being of particular interest because of its role in the evolution, development, and disease pathology of cancer.[1−3] Hsp90 is an ATP-dependent chaperone protein essential for the maturation and activity of a varied group of proteins involved in signal transduction, cell cycle regulation, and apoptosis.[4,5] The ATPase activity can be inhibited with some selectivity by natural product antibiotics such as geldanamycin and its derivatives 17-AAG and 17-DMAG or radicicol and its oxime derivatives (Figure 1).[6] In vivo and clinical data with 17-AAG supports the hypothesis that the Hsp90 family may be an appropriate target for anticancer drug development.[7−11]

Structures of the N-terminal domain of human Hsp90α have been published as unliganded protein and in complex with a variety of inhibitors.[6,12] A seven-stranded β sheet forms the backbone of the protein, and four α helices are arranged such that they form a compact cavity in which resides the ATP binding site.

There has been significant recent interest in the identification of small-molecule Hsp90 inhibitors,[13] and this includes our report of the discovery of a novel series based on a pyrazole template with pendant aryl groups. Discovery of this series was made via a high-throughout screen using an ATPase assay[14,15] and identified CCT018159 (**1**, Table 1), which exhibited activity in the enzyme ATPase activity assay. The structure of this compound bound to Hsp90 guided the design of a fluorescence polarization (FP) assay,[16] allowing the measurement of binding competition with a fluorescent probe. Importantly, **1** inhibited the proliferation of HCT116 human colon tumor cells with the expected pharmacodynamic (PD) "signature" of up-regulation of Hsp70 and down-regulation of one of Hsp90's important client protiens, in this case Raf-1.[2,17]

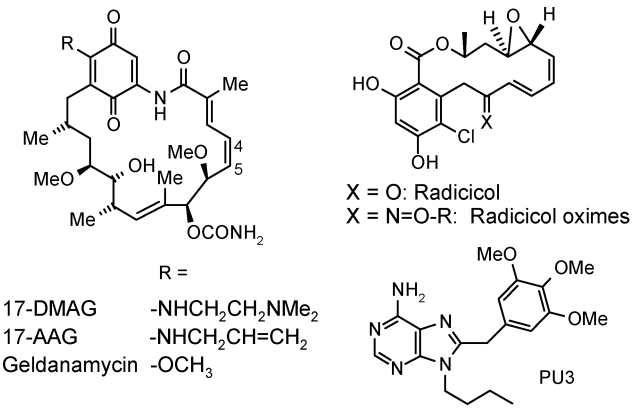

Figure 1. Structures of known Hsp90 inhibitors.

Even though the potency of **1** was better than 17-AAG in the FP binding assay and ATPase functional assay, this did not translate to potent inhibition of HCT116 cell proliferation (Table 1). The GI_{50} of 0.16 μM for 17-AAG is surprisingly low and has been the subject of much discussion in the literature, and one report suggests that this better than expected potency is due to accumulation within the cell.[19]

Herein we report potent derivatives of **1** discovered through a structure-driven design paradigm. One of these new compounds inhibits the proliferation of tumor cells with potency close to that of 17-AAG and represents one of the first small-molecule inhibitors of Hsp90 to be described that demonstrates the required potency and potential to become a clinical candidate.

Information gained from the crystal structure of **1** bound to the N-terminal domain of human Hsp90[14,17,20] was used to drive the lead development program (Figure 2). The structure is essentially identical to the previously reported structure bound to the N-terminal of yeast Hsp90α.[17] The resorcinol groups are clearly central to the binding mode of the compound, particularly the 2′-hydroxyl, which makes a hydrogen bond to the residue Asp93. A key water molecule at the base of the pocket interacts with Asp93 and the pyrazole N2 of the inhibitor. This water is part of a network with Asp93 and two other waters that are seen in all reported crystal structures of Hsp90. The ethyl group on the resorcinol ring of **1** fills a small lipophilic pocket that, upon binding of the weak inhibitor PU3,[21−23] can undergo a major conformational rearrangement to accommodate much bigger lipophilic groups. This binding mode is entirely consistent with the work of Kreusch et al. who have published the crystal structures of two dihydroxyphenylpyrazoles bound to human N-terminal Hsp90α.[24] Further analysis of the crystal structure of

* To whom correspondence should be addressed. Phone: +44 1223 895 313. Fax: +44 1223 895 556. E-mail: m.drysdale@vernalis.com.
† Vernalis Ltd.
‡ The Institute of Cancer Research.

10.1021/jm050355z CCC: $30.25
Published on Web 06/02/2005

Table 1. Biological Data for Hsp90 Inhibitors

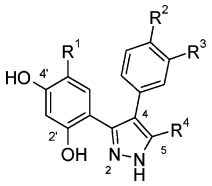

compd	R^1	R^2	R^3	R^4	FP IC_{50} (μM)[b]	ATPase IC_{50} (μM)[a,b]	GI_{50} (μM)[b]
17-AAG					1.27	13.4	0.16
radicicol					0.15	0.20	0.13
1	Et	$-O(CH_2)_2O-$		Me	0.28	5.70	5.8
2	H	$-O(CH_2)_2O-$		Me	4.73	23.0	34.8
3	Cl	$-O(CH_2)_2O-$		Me	0.21	0.65	14.9
4	H	OMe	H	Me	4.40	36.9	33.3
5	Br	OMe	H	Me	0.062	1.90	6.1
6	Cl	OMe	H	Me	0.150	1.7	6.7
7	Cl	OMe	H	COOH	0.51	2.3	>80
8	Cl	OMe	H	$CONH_2$	0.053	0.42	1.1
9	Cl	OMe	H	CONHMe	0.039	0.11	0.68
10	Br	OMe	H	CONHEt	0.070	0.390	0.938
11	Cl	OMe	H	CONHEt	0.025	0.14	0.26
12	Cl	OMe	H	$CONH^iPr$	0.12	1.5	1.9

[a] ATPase activity determined with full length yeast Hsp90 protein. [b] GI_{50}, FP, and ATPase IC_{50} values are averages of at least $n = 2$.

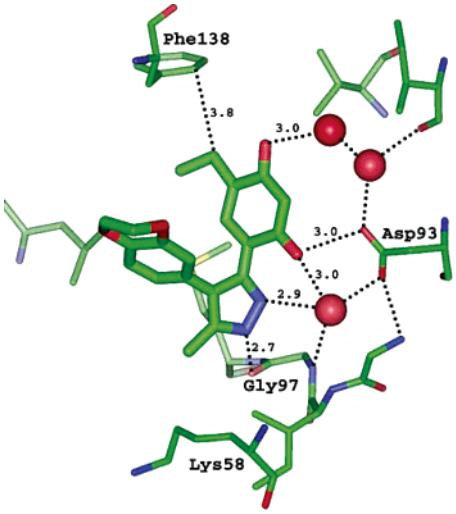

Figure 2. X-ray structure of **1** bound to the ATP binding site of human Hsp90α.

1 revealed that the 4-aryl group was pointing toward the solvent in a quite open part of the binding site, providing little potential for potency gains.[17]

Although the 5-methyl group is located in another solvent channel, it is closer to the protein and there are a number of potential interaction sites that could be accessed by substituents at this point.

The most attractive group to interact with is the carbonyl oxygen of Gly97, located less than 4 Å away from the 5-methyl carbon. This hydrogen bond acceptor is 2.7 Å from the pyrazole's N1, but the interaction is out of the plane of the peptide bond, leaving the lone pairs on the oxygen free to interact with other hydrogen bond donors. Amides (−CONHR), methylamines ($-CH_2$-NHR) and methyl alcohol ($-CH_2OH$) are examples of C5 derivatives theoretically able to form hydrogen bonds with this atom of the backbone of the protein with the correct geometry. The second site of interest in the vicinity of the 5-methyl is a small solvent-exposed hydrophobic patch formed by the side chain of Ile96 and

Scheme 1[a]

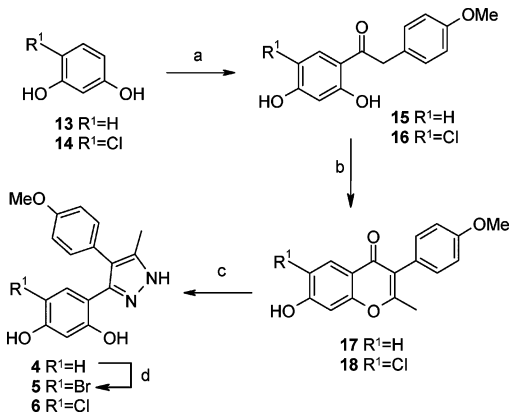

[a] Reagents and conditions: (a) 4-methoxyphenylacetic acid, $BF_3{\cdot}OEt_2$, 90 °C, 90 min; (b) Ac_2O, K_2CO_3, DMF, 115 °C, 90 min; (c) hydrazine hydrate, EtOH, 78 °C, 5 h; (d) $BnNMe_3^+Br_3^-$, DCM, room temp, 90 min.

the aliphatic chain of Lys58. This could make favorable hydrophobic interactions with apolar groups provided by a ligand. Finally, there are several charged side chains between 6 and 12 Å away from the 5-methyl carbon (in order of increasing distance: Lys58, Asp102, His154, Glu62, and Lys69) that could form polar interactions with relatively large substituents. However, owing to the solvation effect and the flexible nature of the side chains of these residues, we believe that it is highly unlikely that this would yield increased potency. On the basis of this analysis of the structure, we gave priority to appending a hydrogen bond donor from the pyrazole 5-position, which we anticipated would result in a new hydrogen bond to the backbone of the protein.

The synthesis of **1**−**3** in Table 1 has been described previously[17,18] (**1** and **2** are also commercially available; see Supporting Information), and the same synthetic route was utilized (Scheme 1) for the synthesis of **4**−**6**. Freidel−Crafts acylation of phenols **13** and **14** afforded the acetophenone derivatives **15** and **16**, which were converted to the chromen-4-ones **17** and **18**. Reaction with hydrazine hydrate afforded the 2,4-dihydroxyphenylpyrazole compounds described. The data for this initial set of compounds (Table 1) demonstrate the importance of the substituent R^1 being lipophilic in nature, with R^1 being chloro and ethyl appearing to afford more potent binding than the corresponding unsubsituted compound (**1** and **3** vs **2**). Replacement of the ethylenedioxyaryl group of **1**−**3** with the 4-methoxyaryl group of **4**−**6** does not have significant effect on the binding as previously predicted on the basis of the available structural information.

We selected an amide as the moiety to incorporate the requisite hydrogen bond donor functionality at the 5-position of the pyrazole. The synthesis of amide compounds **8**, **9**, **11**, and **12** was achieved from carboxylic acid **7** via a standard coupling protocol (Scheme 2). The carboxylic acid **7** was itself prepared from chromene **19** by the route outlined in Scheme 1 using chlorooxoacetic acid methyl ester in place of acetic anhydride in step b. Bromo analogue **10** was prepared in an analogous method to compound **5** from the corresponding $R^1 = H$ series.

Data presented in Table 1 show that the new compounds **8**−**12** display high binding affinity, as evident

Scheme 2[a]

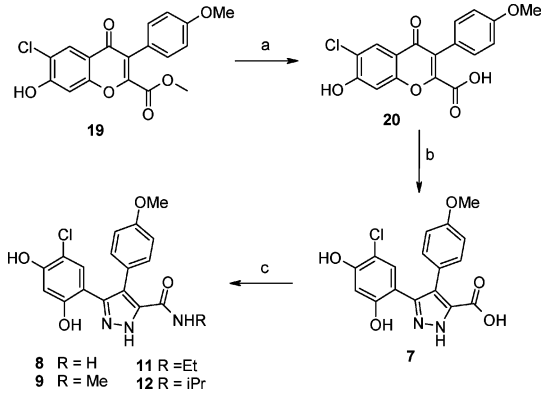

[a] Reagents and conditions: (a) $NaHCO_3$(aq), MeOH, 65 °C, 5 h; (b) hydrazine hydrate, EtOH, 78 °C, 5 h; (c) RNH_2, HOBt, EDCI, DCM, NMM, room temp, 18 h; (d) $BnNMe_3^+Br_3^-$, MeCN, DMF.

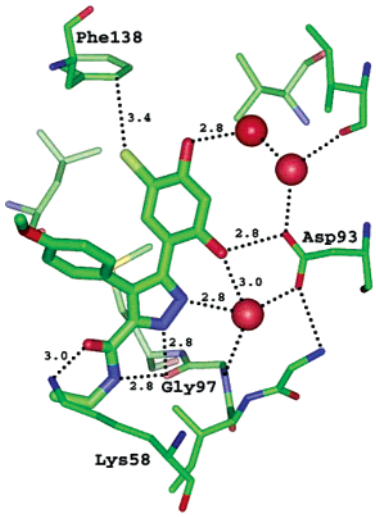

Figure 3. X-ray structure of **11** bound to the ATP binding site of human Hsp90α.[25]

from the FP IC_{50} values. More importantly, however, the amides **8**−**12** now exhibit significantly improved potency in the inhibition of growth of HCT116 cells, with **11** (VER-49009) displaying a value close to that of 17-AAG. Interestingly the bromo analogue **10** is 3-fold less active in all assays compared to **11**.

These changes in binding potency can be rationalized by analysis of the crystal structure of **11** bound to Hsp90 (Figure 3). Key aspects of the binding mode such as the resorcinol hydrogen bonding with the Asp93 and waters remain identical to **1**. As predicted from modeling, the new amide group has made a hydrogen bond with Gly97. This new interaction satisfactorily explains the tighter binding of the amide series. It is interesting to note that the flexible Lys58 residue makes a secondary H-bond interaction with the carbonyl moiety of the amide in **11**. It is reported that the carboxyl groups of 5-carboxy-2′,4′-dihydroxyphenylpyrazoles make a salt bridge with Lys58; however, this interaction did not appear to have a significant effect on binding potency.[24] This is in agreement with the binding affinity for **7** and is not surprising because the side chain of Lys58 is completely solvent-exposed and unconstrained. Thus, any interaction made by its amino group will be counteracted by major solvation and entropic penalties. It is highly probable therefore that the increased

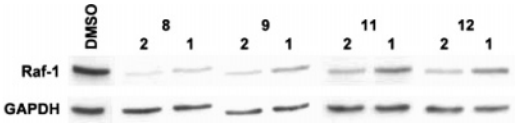

Figure 4. Raf-1 down-regulation following inhibition of Hsp90 by **8**, **9**, **11**, and **12**. HCT116 cells were exposed to 1 × GI_{50} or 2 × GI_{50} **8**, **9**, **11**, and **12** for 48 h, and Raf-1 levels were determined by Western blotting. GAPDH was used to confirm equal loading.

potency seen with the 5-amides is due to the interaction with the key residue Gly97, and this is further corroborated by structural data from other amides from this series that do not make an interaction with Lys58.

To add support to the premise that these new compounds exert their antiproliferate effects via inhibition of Hsp90, we studied the effect of compounds **8**, **9**, **11**, and **12** on the PD marker Raf-1 (a known client of Hsp90 and down-regulated upon Hsp90 inhibition) and the cochaperone Hsp70 (which is up-regulated upon Hsp90 inhibition).[2]

As shown in Figure 4, exposure of HCT116 cells to amides **8**, **9**, **11**, and **12** caused significant reduction in cellular levels of Raf-1 at concentrations equal to the concentration that caused cell growth arrest. Up-regulation of Hsp70 (measured using an Hsp70 specific ELISA) was also observed at similar concentrations (data not shown), and **11** caused a decrease in cellular levels of the client protein CDK4 (data not shown). These results are consistent with the observed effects on cellular growth arrest being through inhibition of cellular Hsp90.

In conclusion, we have discovered a new series of small-molecule Hsp90 inhibitors that display inhibition of cell proliferation similar to clinically evaluated 17-AAG. We have determined a crystal structure of the most potent new compound (**11**) bound to the target enzyme, rationally explaining the observed improvements. Further reports will describe structure−activity relationships in the wider series.

Acknowledgment. The authors are grateful to Adam Hold for compound purification and analysis, Heather Simmonite for NMR results, and Joanne Wayne and Kate Grant for assay determinations.

Supporting Information Available: Synthetic procedures with supporting spectral and HPLC data for **4**−**12** and key parameters relating to X-ray crystallography and methods of protein production. This material is available free of charge via the Internet at http://pubs.acs.org.

References

(1) Jolly, C.; Morimoto, R. I. Role of the heat shock response and molecular chaperones in oncogenesis and cell death. *J. Natl. Cancer Inst.* **2000**, *92*, 1564−1572.
(2) Maloney, A.; Workman, P. HSP90 as a new therapeutic target for cancer therapy: the story unfolds. *Expert Opin. Biol. Ther.* **2002**, *2*, 3−24.
(3) Workman, P. Overview: Translating Hsp90 biology into Hsp90 drugs. *Curr. Cancer Drug Targets* **2003**, *3*, 297−300.
(4) Pearl, L. H.; Prodromou, C. Structure and in vivo function of Hsp90. *Curr. Opin. Struct. Biol.* **2000**, *10*, 46−51.
(5) Young, J. C.; Moarefi, I.; Hartl, F. U. Hsp90: a specialized but essential protein-folding tool. *J. Cell Biol.* **2001**, *154*, 267−273.
(6) Roe, S. M.; Prodromou, C.; O'Brien, R.; Ladbury, J. E.; Piper, P. W.; Pearl, L. H. Structural basis for inhibition of the Hsp90 molecular chaperone by the antitumour antibiotics radicicol and geldanamycin. *J. Med. Chem.* **1999**, *42*, 260−266.

(7) Banerji, U.; O'Donnell, A.; Scurr, M.; Benson, C.; Hanwell, J.; Clark, S.; Raynaud, F.; Turner, A.; Walton, M.; Workman, P.; Judson, I. Phase I trial of the heat shock protein 90 (HSP90) inhibitor 17-allylamino 17-demethoxygeldanamycin (17AAG). Pharmacokinetic (PK) profile and pharmacodynamic (PD) endpoints. *Proc. Am. Soc. Clin. Oncol.* **2001**, *20*, 82a.
(8) Egorin, M. J.; Zuhowski, E. G.; Rosen, D. M.; Sentz, D. L.; Covey, J. M.; Eiseman, J. L. Plasma pharmacokinetics and tissue distribution of 17-(allylamino)-17-demethoxygeldanamycin (NSC 330507) in CD2F1 mice1. *Cancer Chemother. Pharmacol.* **2001**, *47*, 291−302.
(9) Egorin, M. J.; Lagattuta, T. F.; Hamburger, D. R.; Covey, J. M.; White, K. D.; Musser, S. M.; Eiseman, J. L. Pharmacokinetics, tissue distribution, and metabolism of 17-(dimethylaminoethylamino)-17-demethoxygeldanamycin (NSC 707545) in CD2F1 mice and Fischer 344 rats. *Cancer Chemother. Pharmacol.* **2002**, *49*, 7−19.
(10) Munster, P. N.; Tong, L.; Schwartz, L.; Larson, S.; Kenneson, K.; De La Cruz, A.; Rosen, N.; Scher, H. Phase I trial of 17-(allylamino)-17-demethoxygeldanamycin (17AAG) in patients (Pts) with advanced solid malignancies. *Proc. Am. Soc. Clin. Oncol.* **2001**, *20*, 83a.
(11) Soga, S.; Sharma, S. V.; Shiotsu, Y.; Shimizu, M.; Tahara, H.; Yamaguchi, K.; Ikuina, Y.; Murakata, C.; Tamaoki, T.; Kurebayashi, J.; Schulte, T. W.; Neckers, L. M.; Akinaga, S. Stereospecific antitumor activity of radicicol oxime derivatives. *Cancer Chemother. Pharmacol.* **2001**, *48*, 435−445.
(12) Stebbins, C. E.; Russo, A. A.; Schneider, C.; Rosen, N.; Hartl, F. U.; Pavletich, N. P. Crystal structure of an Hsp90−geldanamycin complex: targeting of a protein chaperone by an antitumor agent. *Cell* **1997**, *89*, 239−250.
(13) (a) Dymock, B. W.; Drysdale, M. J.; MacDonald, E.; Workman, P. Inhibitors of Hsp90 and Other Chaperones for the Treatment of Cancer. *Expert Opin. Ther. Pat.* **2004**, *14*, 837−847. (b) Llauger, L.; Huazhong, H.; Kim, J.; Aguirre, J.; Rosen, N.; Peters, U.; Davies, P.; Chiosis, G. Evaluation of 8-Arylsulfanyl, 8-arylsulfoxyl, and 8-arylsulfonyl adenine derivatives as inhibitors of the heat shock protein 90. *J. Med. Chem.* **2005**, *48*, 2892−2905 (c) Drysdale, M. J.; Dymock, B. W.; Barril-Alonso, X.; Workman, P.; Pearl, L. H.; Prodromou, C.; MacDonald, E. Preparation of 3,4-diarylpyrazoles as inhibitors of heat shock protein 90 (Hsp90) and their use in the therapy of cancer. WO 2003/03055860, 2003. (d) Kasibhatla, S. R.; Boehm, M. F.; Hong, K. D.; Biamonte, M. A.; Shi, J.; Le Brazidec, J. Y. Novel heterocyclic compounds as Hsp90 inhibitors. WO 2005/028434, 2005. (e) Vilenchik, M.; Solit, D.; Basso, A.; Huezo, H.; Lucas, B.; He, H.; Rosen, N.; Spampinato, C.; Modrich, P.; Chiosis, G. Targeting wide-range oncogenic transformation via PU24FCl, a specific inhibitor of tumor Hsp90. *Chem. Biol.* **2004**, *11*, 787−797.
(14) Aherne, G. W.; Maloney, A.; Sharp, S.; Clark, P.; Walton, M.; Hardcastle, A.; Boxall, K.; Richards, J.; Rowlands, M.; Newbatt, Y.; Raynaud, F.; Smith, N.; Nutley, B.; McDonald, E.; James, K.; Cheung, J.; Matthews, T.; Roe, M.; Prodromou, C.; Pearl, L.; Workman, P. Discovery of a novel synthetic inhibitor of the Hsp90 molecular chaperone. *Proc. Am. Assoc. Cancer Res.* **2003**, *44*, 915.
(15) Aherne, G. W.; Maloney, A.; Prodromou, C.; Rowlands, M. G.; Hardcastle, A.; Boxall, K.; Clarke, P.; Walton, M. I.; Pearl, L.; Workman, P. Assays for HSP90 and inhibitors. In *Novel Anticancer Drug Protocols*; Buolamwini, J. K., Adjei, A. A., Eds.; Methods in Molecular Medicine, Vol. 85; Humana Press, Inc.: Totowa, NJ, 2003; pp 149−161.
(16) Howes, R.; Barril, X.; Dymock, B. W.; Grant, K.; Northfield, C. J.; Robertson, A.; Surgenor, A.; Wayne, J.; Wright, L.; James, K.; Matthews, T.; Cheung, K.-M.; McDonald, E.; Workman, P.; Drysdale, M. J. *J. Biol. Chem.*, submitted.
(17) Cheung, K.-M.; Matthews, T.; James, K.; Rowlands, M.; Boxall, K.; Sharp, S.; Maloney, A.; Roe, R.; Prodromou, C.; Pearl, L. H.; Aherne, W.; McDonald, E.; Workman, P. The identification, synthesis, protein crystal structure and in vitro biochemical evaluation of a new class of Hsp90 inhibitors. *Bioorg. Med. Chem. Lett.*, in press.
(18) Khilya, V. P.; Aitmambetov, A.; Ismailov, M.; Grishko, L. G. Synthetic and modified isoflavanoids XV. Interaction of synthetic analogs of isoflavones with hydrazine hydrate and its derivatives. *Chem. Nat. Compd.* **1994**, *30*, 580−583.
(19) Chiosis, G.; Huezo, H.; Rosen, N.; Mimnaugh, E.; Whitesell, L.; Neckers, L. 17AAG: Low target binding affinity and potent cell activity—Finding an explanation. *Mol. Cancer Ther.* **2003**, *2*, 123−129.
(20) Smith, N. F.; Hayes, A.; James, K.; Matthews, T.; Nutley, B.; McDonald, E.; Dymock, B.; Drysdale, M.; Raynaud, F. I.; Workman, P. Pharmacokinetic and metabolism studies of a novel synthetic series of heat shock protein 90 (Hsp90) inhibitors. *Clin. Cancer Res.* **2003**, *9*, 239.
(21) Chiosis, G.; Timaul, M. N.; Lucas, B.; Munster, P. N.; Zheng, F. F.; Sepp-Lorenzino, L.; Rosen, N. A small molecule designed to bind to the adenine nucleotide pocket of Hsp90 causes HER2 degradation and the growth arrest and differentiation of breast cancer cells. *Chem. Biol.* **2001**, *8*, 289.
(22) Dymock, B.; Barril, X.; Beswick, M.; Collier, A.; Davies, N.; Drysdale, M.; Fink, A.; Fromont, C.; Hubbard, R. E.; Massey, A.; Surgenor, A.; Wright, L. Adenine derived inhibitors of the molecular chaperone Hsp90-SAR explained through multiple X-ray structures. *Bioorg. Med. Chem. Lett.* **2004**, *14*, 325−328.
(23) Wright, L.; Barril, X.; Dymock, B. L. S.; Surgenor, A.; Beswick, M.; Drysdale, M.; Collier, A.; Massey, A.; Davies, N.; Fink, A.; Fromont, C.; Aherne, W.; Boxall, K.; Sharp, S.; Workman, P.; Hubbard, R. E. Structure−activity relationships in purine-based inhibitor binding to Hsp90 isoforms. *Chem. Biol.* **2004**, *11*, 775−785.
(24) Kreusch, A.; Han, S.; Brinker, A.; Zhou, V.; Choi, H.-a.; Yun, H.; Lesley, S. A.; Caldwell, J.; Gu, X.-j. Crystal Structure of human Hsp90α-complexed with dihydroxyphenylpyrazoles *Bioorg. Med. Chem. Lett.* **2005**, *15*, 1475−1478.
(25) Atomic coordinates have been deposited with the Protein Data Bank at Rutgers University (http://rcsb.rutgers.edu/pdb/index.html). PDBid codes for **1** and **11** are 2BT0 and 2BSM, respectively.

JM050355Z